NASA TECHNICAL NOTE

NASA TN D-7085

NASA TN D-7085

APOLLO EXPERIENCE REPORT - SPACECRAFT HEATING ENVIRONMENT AND THERMAL PROTECTION FOR LAUNCH THROUGH THE ATMOSPHERE OF THE EARTH

by Robert L. Dotts

Manned Spacecraft Center
Houston, Texas 77058

NATIONAL AERONAUTICS AND SPACE ADMINISTRATION • WASHINGTON, D. C. • MARCH 1973

1. Report No.	2. Government Accession No.	3. Recipient's Catalog No.
NASA TN D-7085		

4. Title and Subtitle	5. Report Date
APOLLO EXPERIENCE REPORT SPACECRAFT HEATING ENVIRONMENT AND THERMAL PROTECTION FOR LAUNCH THROUGH THE ATMOSPHERE OF THE EARTH	March 1973
	6. Performing Organization Code
7. Author(s)	8. Performing Organization Report No.
Robert L. Dotts, MSC	MSC S-350
	10. Work Unit No.
9. Performing Organization Name and Address	914-50-20-12-72
Manned Spacecraft Center Houston, Texas 77058	11. Contract or Grant No.
	13. Type of Report and Period Covered
12. Sponsoring Agency Name and Address	Technical Note
National Aeronautics and Space Administration Washington, D.C. 20546	14. Sponsoring Agency Code

15. Supplementary Notes

The MSC Director waived the use of the International System of Units (SI) for this Apollo Experience Report because, in his judgment, the use of SI Units would impair the usefulness of the report or result in excessive cost.

16. Abstract

An accurate definition of the aerothermodynamic environment of the Apollo spacecraft was necessary to ensure the structural integrity of the spacecraft during the boost phase of the mission. Without an adequate definition of the environment and a provision for thermal protection, the temperature levels and thermal gradients induced in the structure of the spacecraft by the boost-phase aerothermodynamic environment could result in degradation of the structural properties of the spacecraft, degradation of the thermal-control coatings, and excessive thermal stresses in the structure. The techniques that were used to define the aerothermodynamic environment of the Apollo spacecraft during the boost phase and to predict the structural temperatures of the spacecraft are discussed in this report. Also, the wind-tunnel and radiant-heating tests that were used to support the analytical predictions are discussed; the analytical predictions are discussed; the accuracy of the boost-phase heating-analysis techniques is shown by comparing the techniques with flight data. The analytical techniques for predicting heating characteristics and structural temperatures of the spacecraft were adequate for predicting the temperatures of the Apollo spacecraft during the boost phase. Also, the applicability of similar techniques for future spacecraft design and analysis is indicated.

17. Key Words (Suggested by Author(s))	18. Distribution Statement
• Launch Vehicle Configurations • Aerothermodynamics • Thermal Protection • Aerodynamic Heating	

19. Security Classif. (of this report)	20. Security Classif. (of this page)	21. No. of Pages	22. Price
None	None	23	$3.00

* For sale by the National Technical Information Service, Springfield, Virginia 22151

APOLLO EXPERIENCE REPORT
SPACECRAFT HEATING ENVIRONMENT AND THERMAL PROTECTION FOR LAUNCH THROUGH THE ATMOSPHERE OF THE EARTH

By Robert L. Dotts
Manned Spacecraft Center

SUMMARY

An accurate definition of the boost-phase aerothermodynamic environment of the Apollo spacecraft was required for the design of a thermal protection system that would ensure the structural integrity of the spacecraft during the boost phase of an Apollo mission. Without adequate protection, the temperatures and the temperature gradients induced in the spacecraft structure by the boost-phase aerothermodynamic environment would result in an unacceptable degradation of the spacecraft structural properties and thermal-control coatings, significant thermal stresses in the structure, and excessive temperatures in the pyrotechnic charges attached to the structure.

The total Apollo boost-phase thermal protection system of the spacecraft is discussed in this report, and the techniques that were used to predict the boost-phase aerodynamic-heating environment of the spacecraft are discussed briefly. In general, conservative design approaches were used; however, localized failures of several lunar module adapter panels during the Apollo 6 (AS-502) mission caused an extensive reevaluation of the component that resulted in thermal redesign. Extensive analyses and ground tests were performed on this component during the investigation of the AS-502 anomaly. The results of the analyses and tests are discussed in detail. In addition, analytical predictions of structural thermal response to the boost-phase environment are compared with flight data.

INTRODUCTION

The Apollo spacecraft is subjected to substantial boost-phase aerodynamic heating during launch through the atmosphere of the earth. An accurate definition of the effects of this boost-phase aerodynamic-heating environment on the Apollo spacecraft was required to design a thermal protection system that would ensure structural integrity of the spacecraft and subsequent operation of all spacecraft systems and components affected by this thermal environment.

The design of the boost-phase thermal protection system of the Apollo spacecraft involved definition of the boost-phase aerodynamic-heating environment; thermal analysis of the various spacecraft elements during the boost phase to determine the temperature histories of the elements; design of thermal protection systems for the spacecraft elements that would experience excessive temperatures during the boost phase; and ground tests of the various elements of the thermal protection system and flight tests of the integrated thermal protection system to verify the adequacy of the design.

The general boost-phase design considerations of the thermal protection system for the primary Apollo spacecraft components are discussed in this report. Also, the techniques that were used to define the aerodynamic-heating environment are discussed; the basic thermal-analysis techniques and the ground and flight tests that were used to verify the adequacy of the design of the thermal protection system are presented.

SPACECRAFT BOOST-PHASE THERMAL-PROTECTION-SYSTEM CONFIGURATION AND DESIGN CONSIDERATIONS

The primary spacecraft elements that require boost-phase thermal protection are shown in figure 1. The elements include the launch escape system (LES); the boost protective cover (BPC), which covers the command module (CM) during launch; the service module (SM); and the spacecraft/lunar module adapter (SLA), which covers the lunar module.

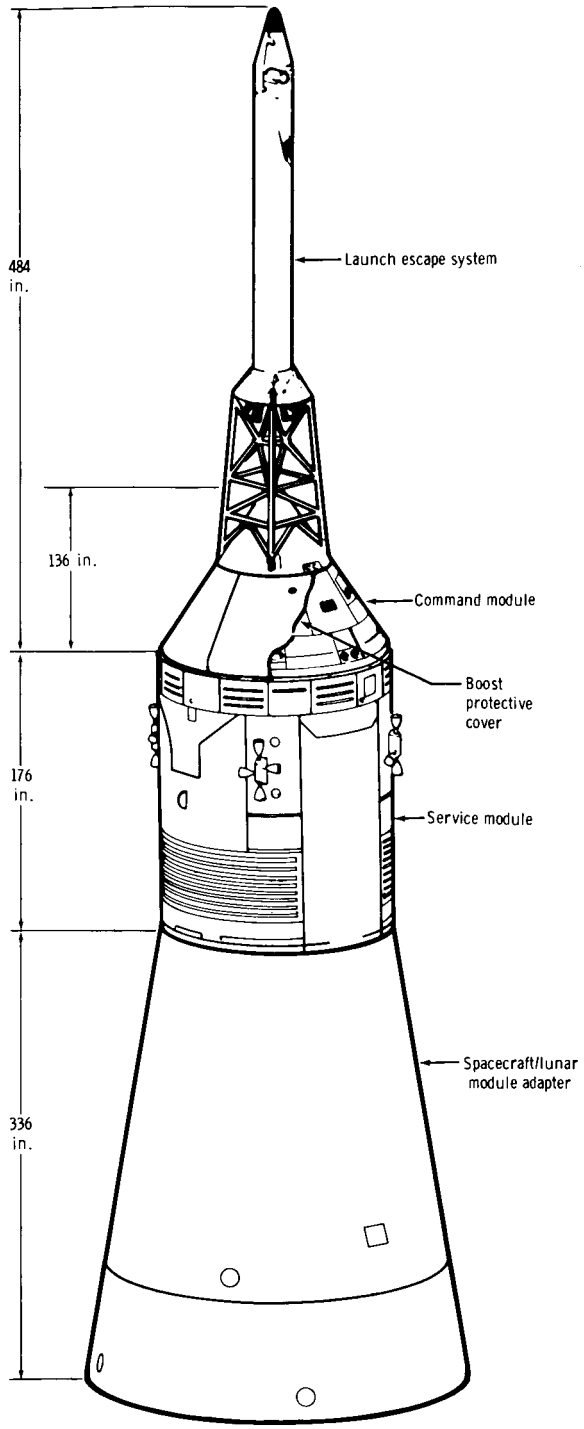

Figure 1. - Spacecraft launch configuration.

Launch Escape System

The purpose of the LES is to remove the CM rapidly from the vicinity of the booster during a boost-phase abort. The LES (fig. 2) consists of a solid-propellant-rocket-motor assembly that contains three rocket motors attached to the forward portion of the CM by a tower structure. The CM BPC is attached to the LES tower structure and provides thermal protection for the CM during the boost phase. The entire LES, including the BPC, is jettisoned near completion of a normal boost phase or an abort.

The legs and crossmembers of the LES tower were covered with Buna-N rubber insulation that was sized to restrict the maximum temperature of the horizontal and vertical titanium leg members to 600° F and the diagonal leg members to 800° F during the design boost-abort phase. The thermal response of a typical vertical leg member (location A in fig. 2) during the AS-503 design boost-phase/abort environment (ref. 1) is shown in figure 3. External corkboard ablative thermal-protection material was used to protect the tower-jettison motor, part of the LES motor, the power-systems and instrumentation wire harness, and the structural skirt from the boost-phase/abort thermal environment. A typical thermal response for the LES motor casing (location B in fig. 2) during the AS-503 design boost-phase/abort environment (ref. 1) is shown in figure 4.

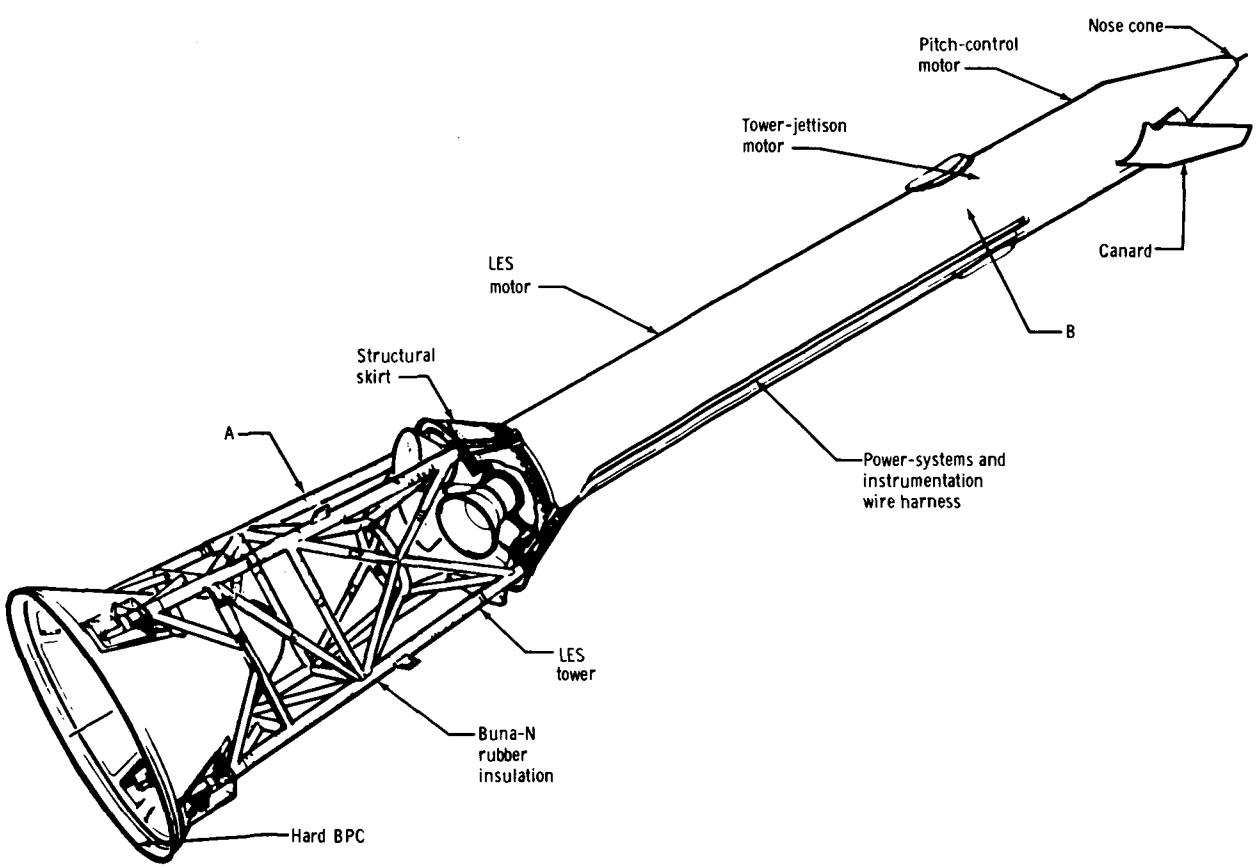

Figure 2. - Launch escape system.

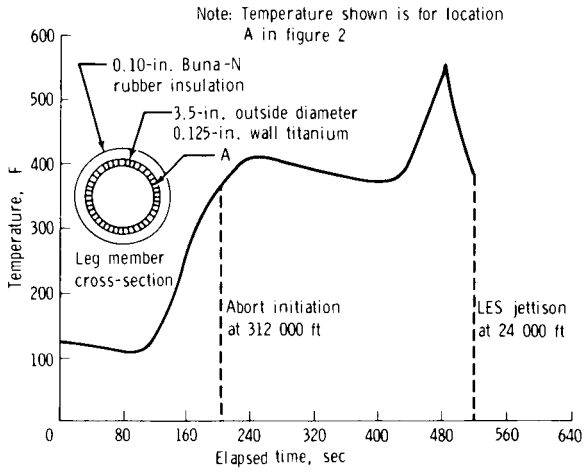

Figure 3. - Thermal response of the LES-tower vertical leg member during the AS-503 design boost-phase/abort environment.

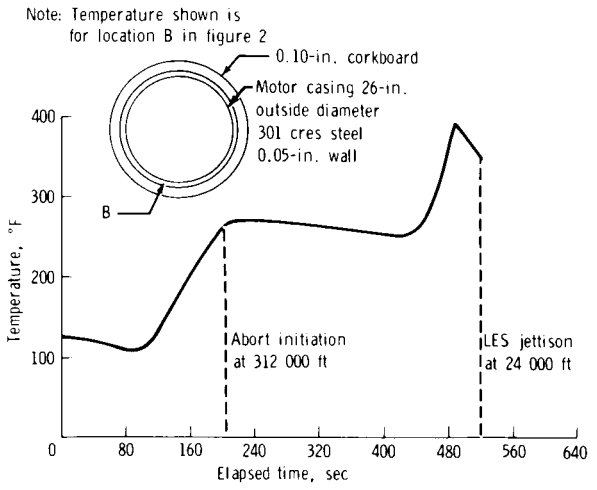

Figure 4. - Thermal response of the LES motor casing during the AS-503 design boost-phase/abort environment.

Command Module

The BPC prevents the CM external thermal-control coating from exceeding 250° F and provides protection from coating contamination during the boost phase. Also, the BPC protects the CM from the high-temperature exhaust of the LES motor during a boost-phase abort. A side view of the BPC is shown in figure 5. The BPC is composed of two sections: a hard cover that is attached to the LES tower legs and a soft cover that is connected to the trailing edge of the hard cover. The hard cover is a phenolic fiber-glass/honeycomb sandwich that is covered with cork thermal-protection material (0.3 inch thick). A typical thermal response for the BPC during the AS-503 design boost-phase/abort environment is shown in figure 6. The temperatures shown are for

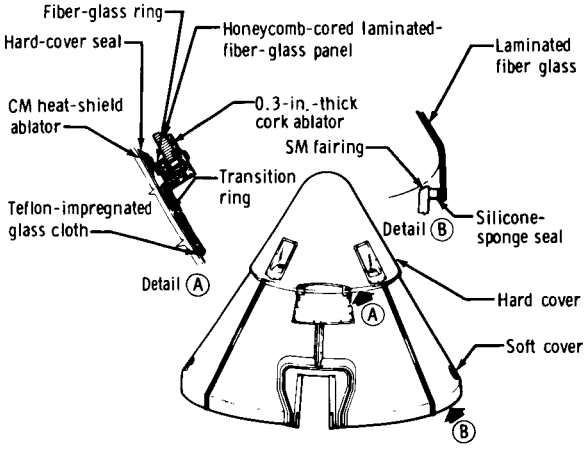

Figure 5. - Boost protective cover.

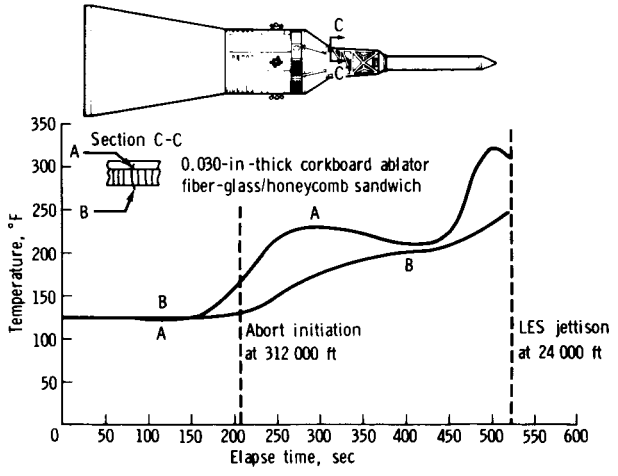

Figure 6. - Thermal response of the hard BPC during the AS-503 design boost-phase/abort environment.

the outer and inner facesheets of the hard-cover fiber-glass/honeycomb sandwich (ref. 1). The soft cover consists of a 0.008-inch-thick Teflon-impregnated glass cloth that is reinforced on the outer surface with a 0.0095-inch-thick nylon fabric. Cork thermal-protection material is bonded to the outer surface of the nylon fabric.

Service Module

The SM (fig. 7) is a cylindrical unit that is composed of an outer shell and an inner concentric core. The resulting annulus is divided into six bays by radial beams. The outer shell is fabricated of 1-inch-thick aluminum-honeycomb panels and is covered with cork thermal-protection material (0.020 to 0.155 inch thick), except in the regions where the environmental control system (ECS) and the electrical power system (EPS) radiators are located. The cork provides protection from boost heating and SM reaction control system (RCS) plume-impingement heating. The cork thickness was sized to maintain the SM honeycomb structure below the design temperature limit of 400° F during boost. The four RCS modules, which protrude from the surface of the SM shell approximately 10 inches, cause flow disturbances that result in increased boost-heating rates in the vicinity of the modules. The cork thicknesses on a representative portion of the SM surface are shown in figure 8. The longitudinal position on the SM is defined, in inches, by X_S. The position X_S = 200 inches corresponds to the lower end of the SM; X_S = 376 inches corresponds to the top of the SM. The circumferential position is defined in terms of angular position measured in degrees from the +Y axis. The thicknesses result from designing for the heating variation over the surface (ref. 1) and from maintaining a maximum temperature of 400° F at all surface points while minimizing the cork weight.

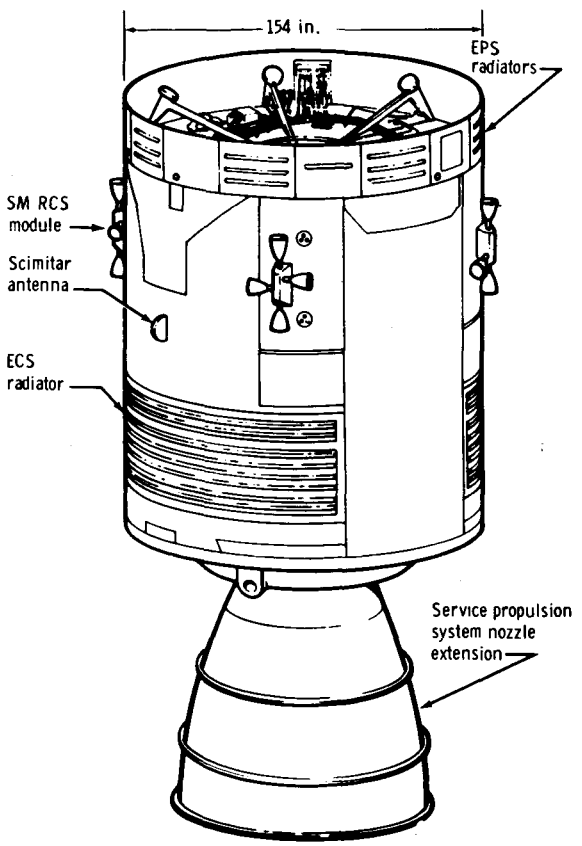

Figure 7. - Service module.

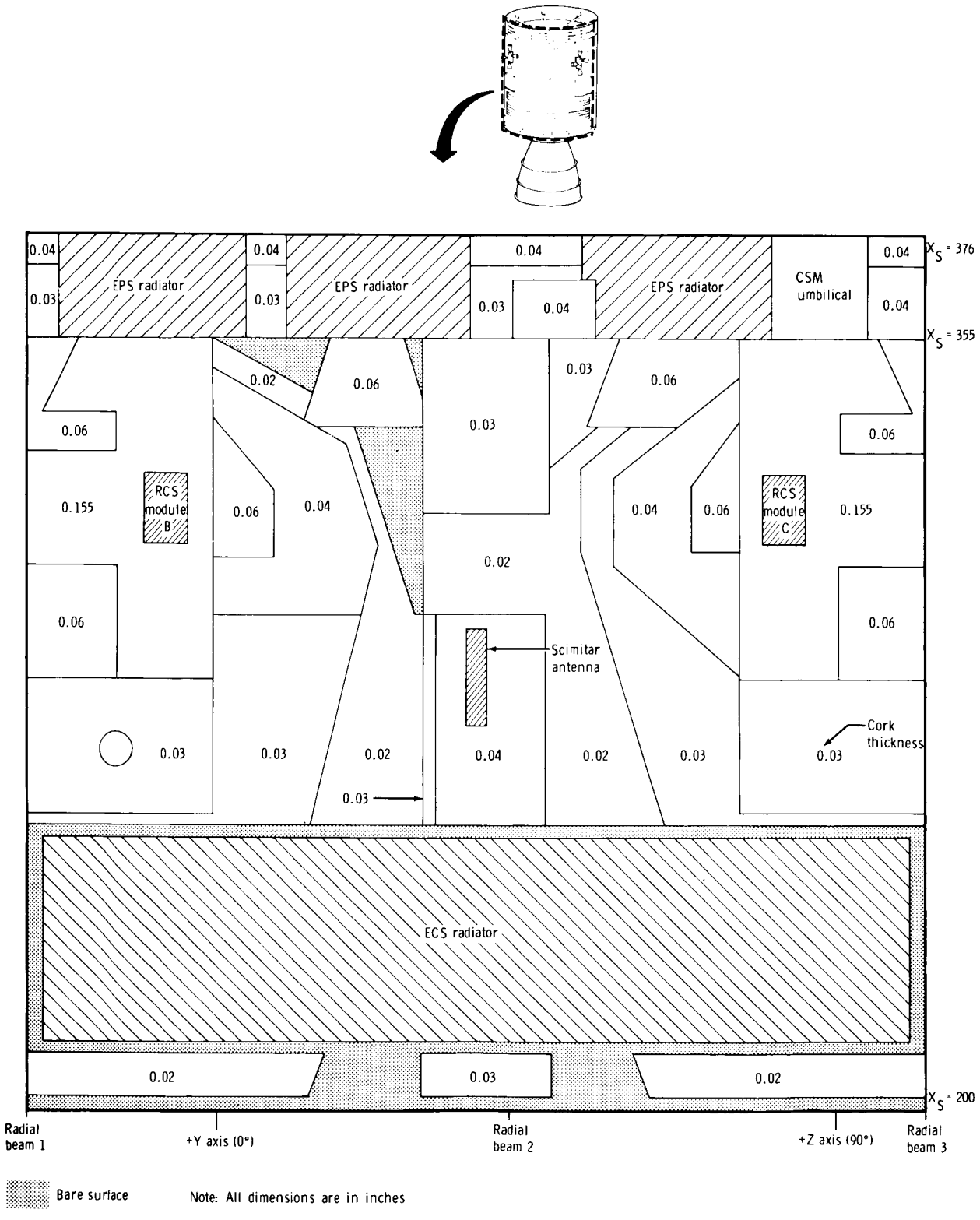

Figure 8. - Block II SM (AS-503 and subsequent spacecraft) cork thermal-protection thickness.

Spacecraft/Lunar Module Adapter

The SLA structure is a truncated conical shell (fig. 9) that is fabricated of 1.7-inch-thick aluminum-honeycomb panels with an outer cover of cork thermal-protection material (0.030 to 0.20 inch thick). Numerous items, such as hinges, antennas, lights, access doors, and structural joints, protrude from the surface of the SLA (fig. 10), causing flow disturbances and localized areas of increased aerodynamic heating. The items were protected by cork or fabricated of material capable of withstanding the localized temperature extremes (ref. 1). The longitudinal position on the SLA is defined, in inches, by X_A. The position X_A = 502 inches corresponds to the lower end of the SLA; X_A = 838 inches corresponds to the top of the SLA. The circumferential position is defined in terms of angular position measured in degrees from the +Y axis.

Initially, the cork thickness was sized to maintain the SLA honeycomb structure below the design temperature limit of 490° F. The 0.030-inch-thick cork (shaded surfaces in fig. 10) was added to Apollo 8 (AS-503) and subsequent adapters because of the AS-502 anomaly. The AS-502 SLA had a localized structural failure of several panels during the boost phase; as a result of the subsequent investigation, the 0.030-inch-thick cork was added to the bare surfaces of the SLA to reduce the temperatures and temperature gradients in the SLA structure.

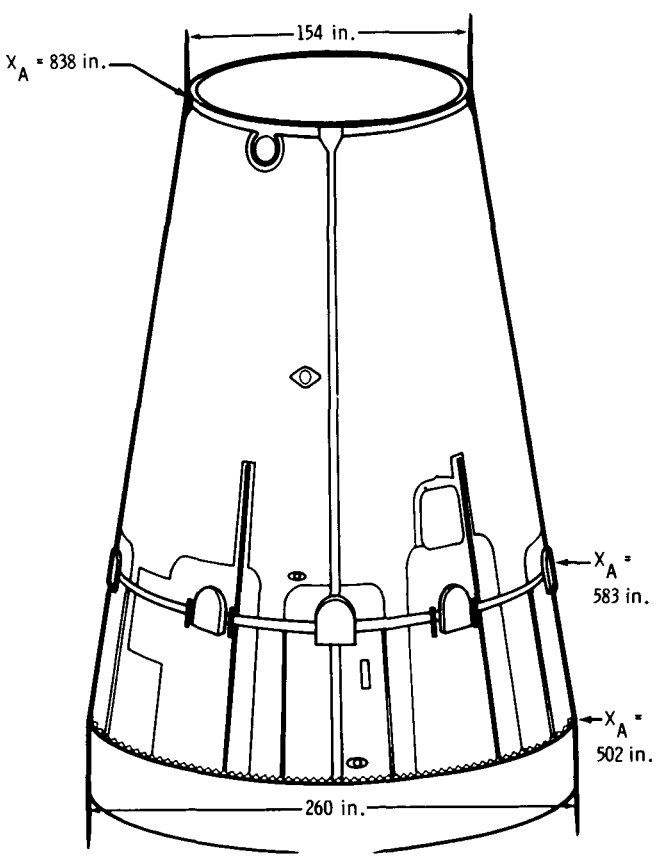

Figure 9. - Spacecraft/lunar module adapter.

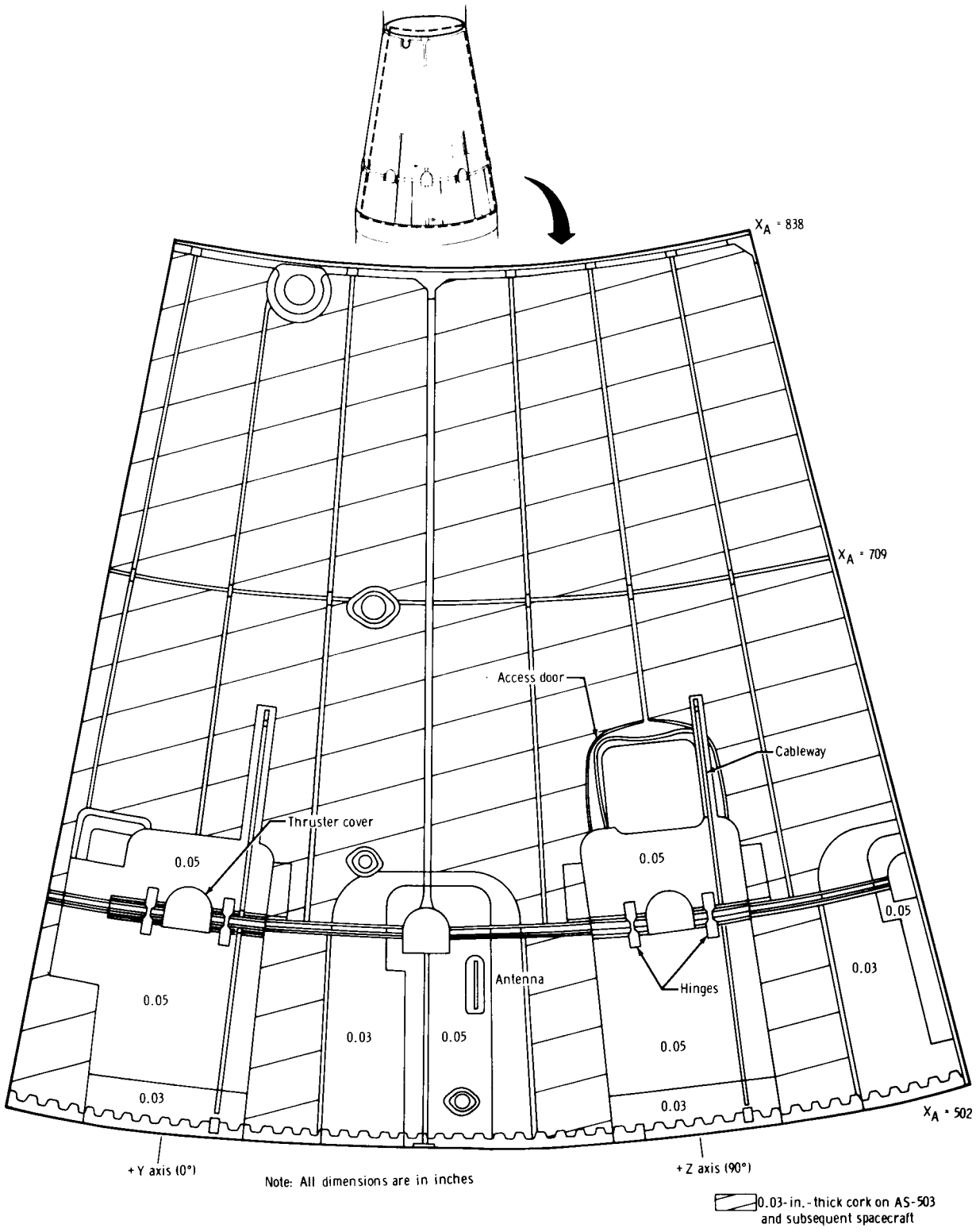

Figure 10. - Cork thermal-protection thickness on the SLA.

THE SM AND SLA BOOST-PHASE AERODYNAMIC-HEATING ENVIRONMENT

A boost-phase aerodynamic-heating computer program that was originally developed and used for Gemini spacecraft boost-heating analysis was used in defining the Apollo spacecraft boost-phase aerodynamic-heating environment. The computer program characterized the flow of air over the vehicle with a normal shock at the nose and an isentropic expansion to local conditions at each specific body station. Eckert's reference-enthalpy method (ref. 2) was used in the computer program with the Blasius skin-friction coefficient (ref. 3) for laminar flow and the Schultz-Grunow skin-friction coefficient (ref. 4) for turbulent flow. The local pressure P_L was determined by using the ratio P_L/P_T and the total pressure P_T behind the normal shock. The local thermodynamic state point was then defined using the entropy behind the normal shock and P_L. The ratio P_L/P_T for the SM and the SLA is a function of Mach number, Reynolds number, vehicle angle of attack, and local body station. Wind-tunnel tests on scale models of the Apollo spacecraft launch configuration were performed to determine the pressure distribution over the vehicle surface for various Mach numbers and Reynolds numbers at 0° angle of attack. Angle-of-attack effects on SM and SLA heating were negligible because of the small angle of attack (nominally less than 1°) for the Apollo vehicle during the heating portion of the nominal boost-phase trajectory. The wind-tunnel model and the pressure-measurement locations are shown in figure 11. Curve fits of the pressure-ratio data for the SM and the SLA are shown in figure 12. Variation of P_L/P_T with Reynolds number was small; therefore, the data could be correlated uniquely with the Mach number. For a given vehicle trajectory and SM or SLA location, time histories for smooth-body heating rate were generated for a range of surface temperatures. The heating rates were used in a thermal-analysis computer program as a function of time and vehicle-surface temperature to calculate transient temperatures at various locations on the SM and the SLA. Time histories for smooth-body heating rate for a typical AS-202 SLA location are shown in figure 13. The specific temperatures used to generate the heating-rate curves of figure 13 were chosen to bracket the expected SLA surface temperatures.

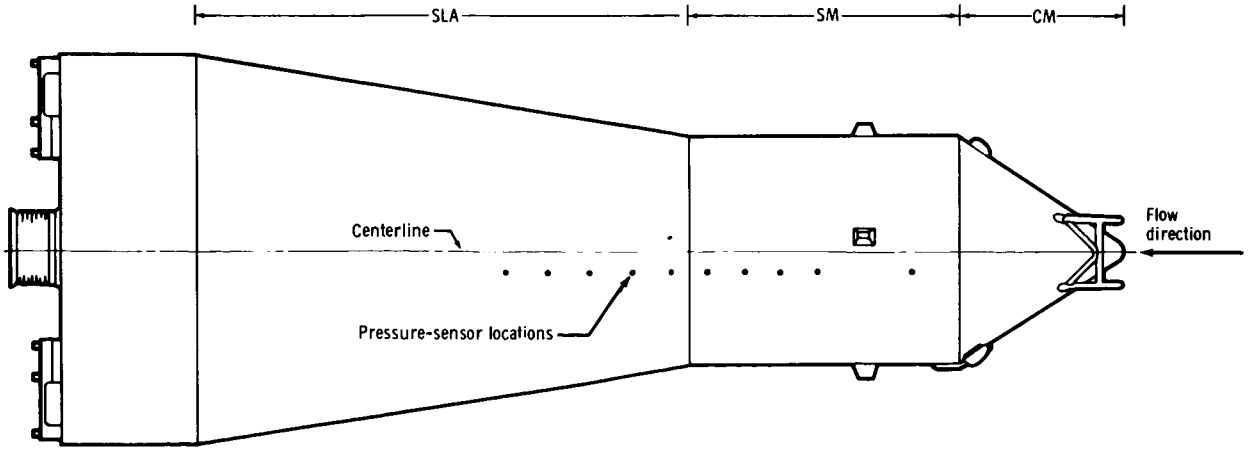

Figure 11. - Wind-tunnel-model configuration and pressure-measurement locations; the model is 0.045 scale.

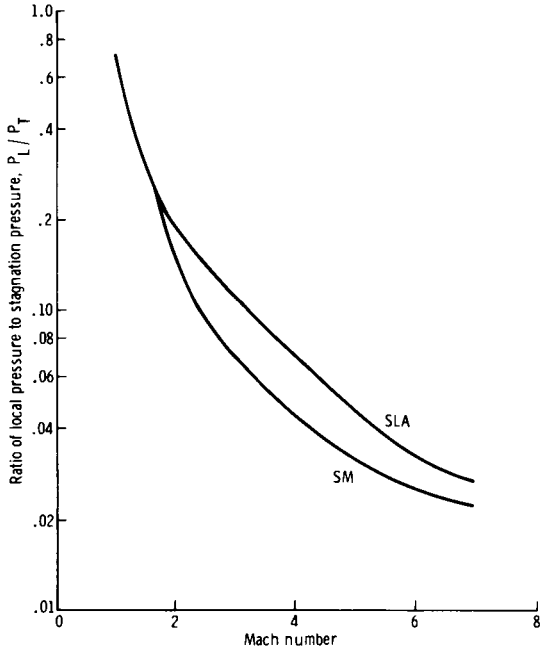

Figure 12. - Ratio of local pressure to stagnation pressure P_L/P_T as a function of Mach number for the SM and SLA.

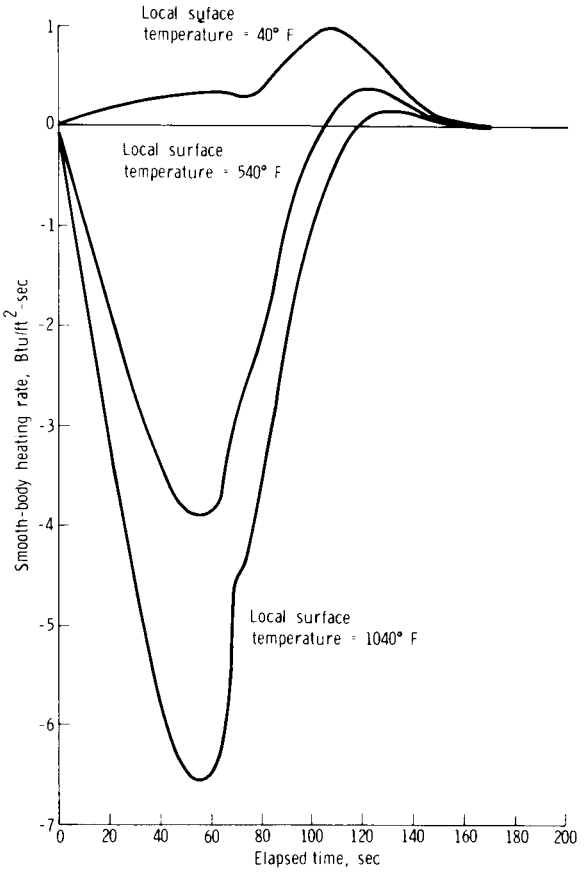

Figure 13. - Time histories for smooth-body heating rate for the AS-202 SLA (station X_A = 775 in.).

The increased heating that was caused by the various flow disturbances on the surfaces of the SM and the SLA was accounted for by using protuberance factors (ratios of the smooth-body heating rate to the local heating rate). The factors were applied as constant multipliers to the smooth-body heating rates throughout the boost-phase trajectory. This conservative approach of using constant factors rather than varying the factors with Mach number was used to ensure adequate design safety margins for the protuberance-affected areas of the spacecraft. Subsequent Apollo flight data indicated that this approach was overly conservative; therefore, Mach-number-varying protuberance factors were used later to verify the adequacy of the SM and the SLA for off-nominal trajectories. The predicted protuberance-factor contours that result from the RCS modules and other protuberances on the surface of the SM are shown in figure 14 (ref. 5). The predicted protuberance-factor contours for two sections of the SLA surface are shown in figures 15 and 16 (ref. 5). The protuberance-factor contours were estimated by using the test data obtained from reference 6 and wind-tunnel data for the Apollo spacecraft configuration.

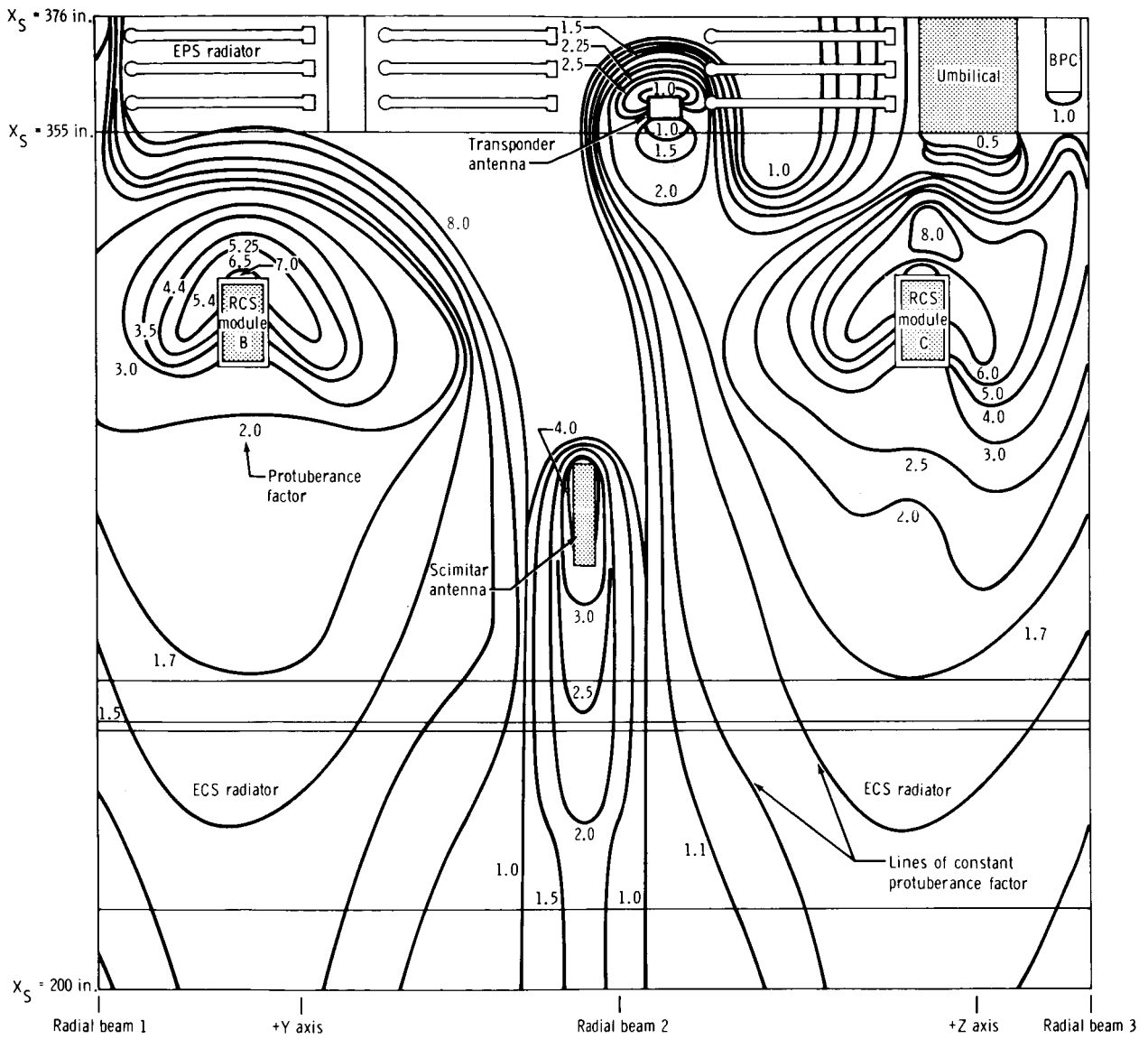

Figure 14. - Typical interference-heating map of protuberance-factor contours for a section of the SM.

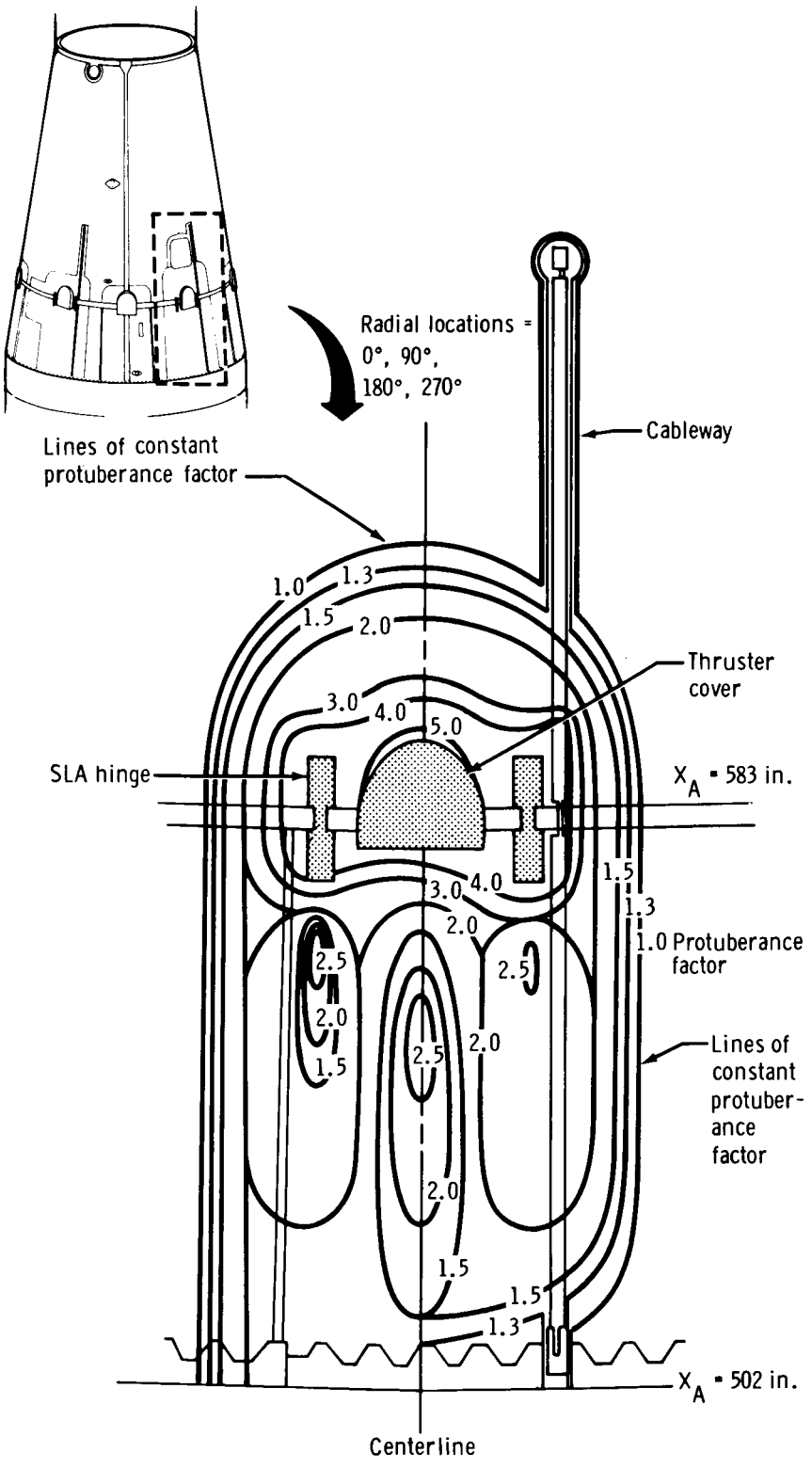

Figure 15. - Local interference-heating map of protuberance-factor contours for SLA hinges, thruster cover, and cableway system.

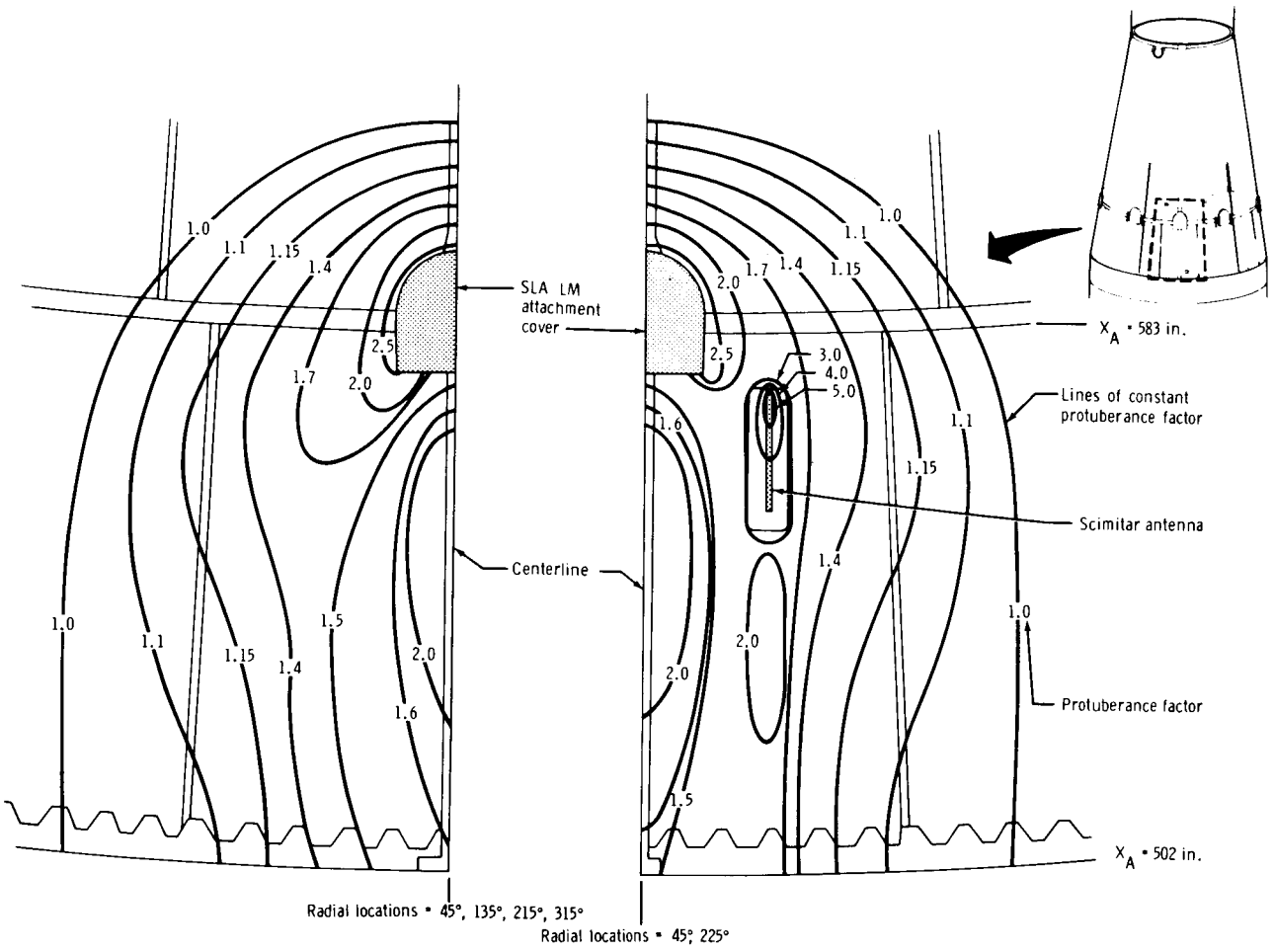

Figure 16. - Local interference-heating map of protuberance-factor contours for SLA/LM attachment cover and scimitar antenna.

BOOST-PHASE THERMAL RESPONSE OF THE SM AND SLA STRUCTURES

Thermal-Mathematical Models and Assumptions

The thermal response of the structure was determined by using the surface-heating-rate histories as boundary conditions for one- and two-dimensional thermal-mathematical models of the structure. Most of the SM and SLA structures are comprised of aluminum-honeycomb-sandwich panels that can be analyzed adequately by using a one-dimensional model. The thermophysical properties of the honeycomb panels were obtained from reference 7. A typical one-dimensional thermal model is shown in figure 17. One-dimensional mathematical models, which are similar to the model shown in figure 17, and two-dimensional mathematical models of more complex SM and SLA structural elements (joints, bulkheads, et cetera) were used for all temperature predictions. Extensive radiant-heating tests were performed to ensure that the one- and two-dimensional mathematical models were adequate. Also, the tests were used to determine the performance of the cork thermal-protection material that was used extensively on the surfaces of the SM and the SLA.

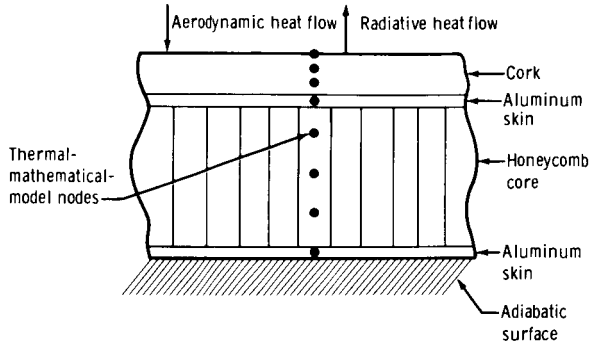

Figure 17. - One-dimensional model of an aluminum-honeycomb panel.

Ground Testing

One-dimensional SLA honeycomb-panel thermal tests. - Thermal tests were performed on 12- by 12-inch, 1.7-inch-thick SLA honeycomb panels to verify the analytical techniques that were used to predict temperatures. Radiant-heating lamps were used to simulate the boost-phase heating history. Lamp voltages were programed so that the bare-surface (without cork) honeycomb outer-facesheet test temperatures matched the analytically predicted temperature history for the AS-503 and subsequent-spacecraft design trajectory. The bare-surface SLA honeycomb-panel thermal response for the AS-503 simulation is shown in figure 18. The inner-honeycomb-surface analytical predictions that resulted from using a one-dimensional thermal model were slightly higher than the measured temperatures. Cork-covered honeycomb panels were subjected to the AS-503 radiant-heating history to assess the cork performance and to determine the accuracy of the analytical predictions. The predicted and measured thermal response for a panel covered with 0.030-inch-thick cork and subjected to the AS-503 radiant-heating history are shown in figure 19. The analytical results that were obtained by using thermophysical-property data for virgin cork agreed well with the test data. The predicted and measured responses for a panel covered with 0.050-inch-thick cork and subjected to the AS-503 heating history are shown in figure 20. The tests demonstrated the adequacy of the analytical temperature-prediction techniques for both bare-surface and cork-covered honeycomb panels in typical Apollo launch environments.

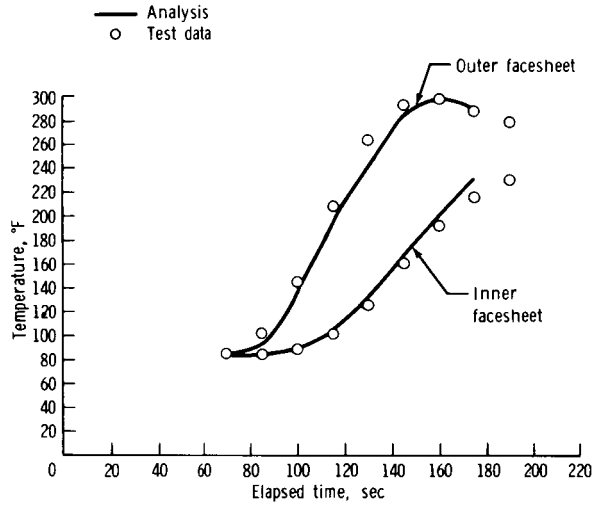

Figure 18. - Thermal response of a bare-surface SLA honeycomb panel to an AS-503 trajectory simulation.

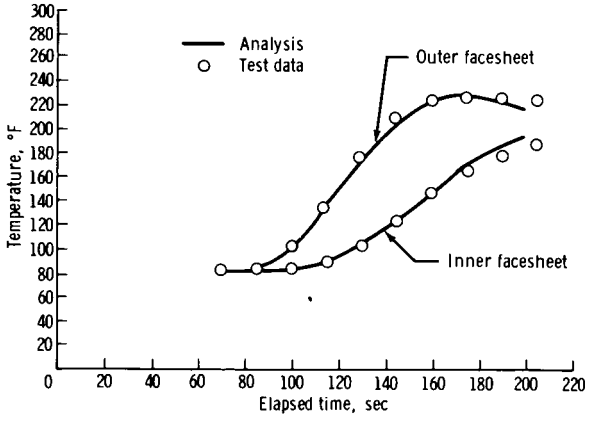

Figure 19. - Thermal response of a cork-covered 0.030-inch-thick SLA honeycomb panel to an AS-503 trajectory simulation.

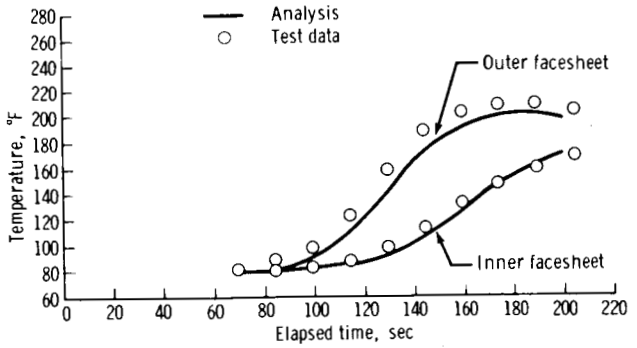

Figure 20. - Thermal response of a cork-covered 0.050-inch-thick SLA honeycomb panel to an AS-503 trajectory simulation.

Two-dimensional SLA-joint thermal tests. - Nine test samples were cut from a structural-test SLA at the locations shown in figure 21. The samples were used to perform radiant-heating tests to assess the temperature gradients in the SLA at the end of first-stage boost and to verify the adequacy of the analytical-prediction techniques. Each panel was subjected to the AS-503 radiant-heating profile that was used in the one-dimensional radiant-heating tests; however, only the data that were obtained from test joint 3 will be discussed in this report. Cross-sectional and top views of the test joint are shown in figures 22 and 23; the thermocouple locations also are shown in figure 23.

The joint was configured with the AS-501 cork pattern (a 0.1-inch-thick layer over only the pyrotechnic joint) and subjected to the heating history of the AS-503 design trajectory. The thermocouple temperatures for the joint after an elapsed time of 150 seconds (the approximate termination of first-stage boost) are shown in figure 24. The two-dimensional thermal-mathematical model (fig. 25) was used to predict the joint temperatures for the same heating profile. The analytical predictions also are shown in figure 24. The correlation is very good, if consideration is given to the complexity of the joint and the uncertainties in the thermal-mathematical model (thermophysical properties, contact resistances, and so forth).

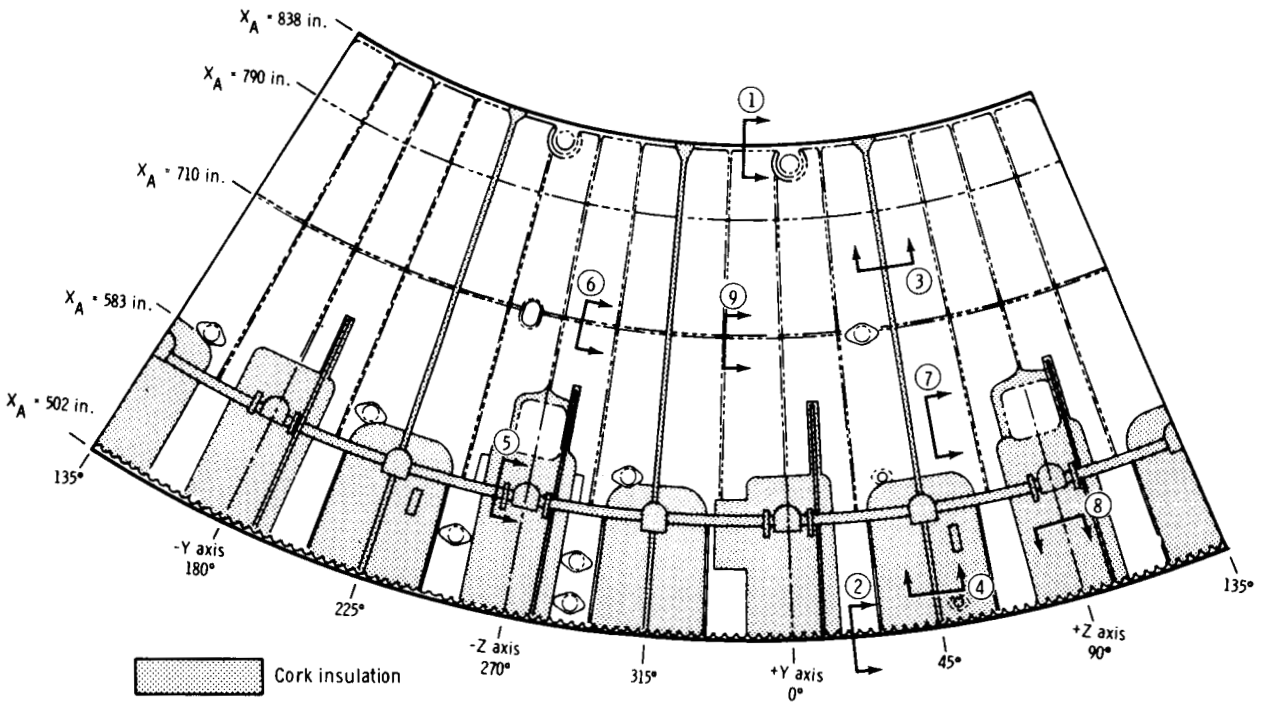

Figure 21. - Spacecraft/lunar module adapter test-joint locations.

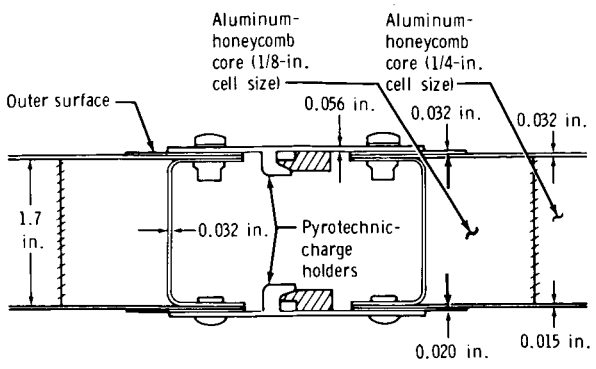

Figure 22. - Cross section of test joint 3 (longitudinal-separation joint between stations X_A = 710 in. and X_A = 750 in.).

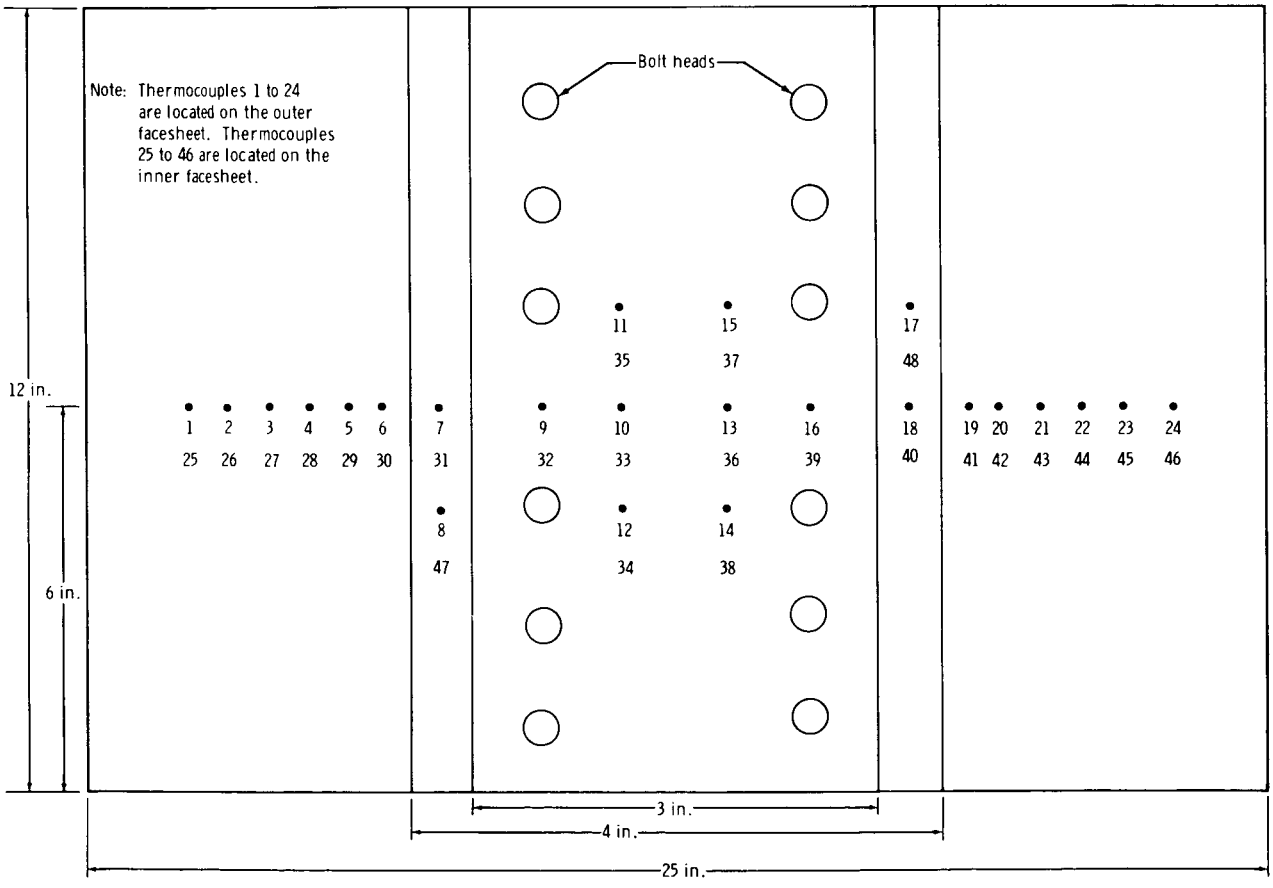

Figure 23. - Top view of test joint 3 (longitudinal-separation joint between stations X_A = 710 in. and X_A = in.) with thermocouple locations.

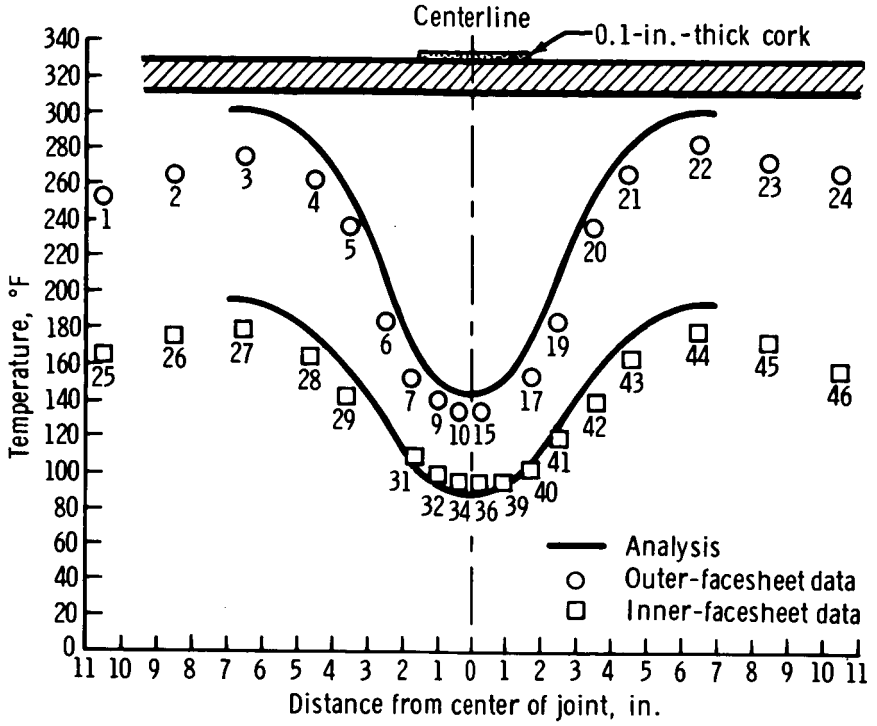

Figure 24. - Temperature distribution for test joint 3 covered with an AS-501 cork pattern and subjected to an AS-503 trajectory simulation.

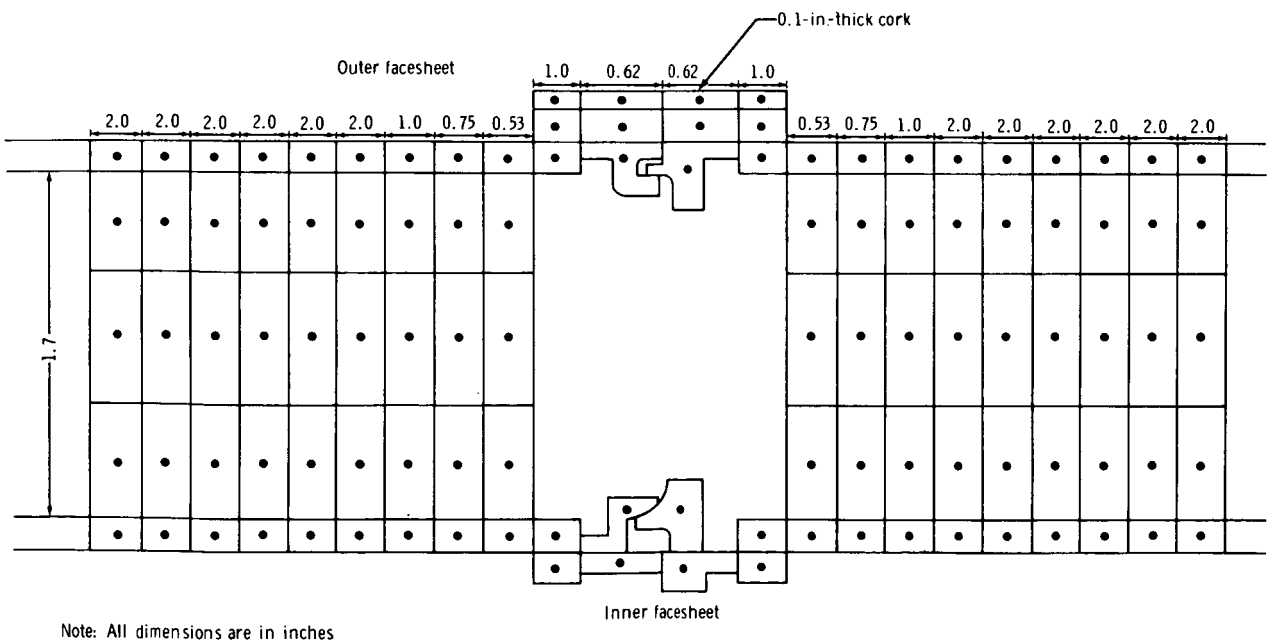

Figure 25. - Thermal-mathematical-model nodes for test joint 3 covered with an AS-501 cork pattern and subjected to an AS-503 trajectory simulation; the diagram is not to scale.

A 0.030-inch-thick cork layer was bonded to the remaining bare surfaces of the panel, which corresponded to a proposed AS-503 SLA cork configuration. The radiant-heating simulation was again performed on the joint to assess the effect of the added 0.030-inch-thick cork on the thermal gradient in the joint. The test results for the configuration are shown in figure 26. The addition of the 0.030-inch-thick cork layer reduced the gradient in the outer facesheet from 140° to 90° F. The results of the two-dimensional SLA-joint thermal tests were used to define the temperatures and temperature gradients in the SLA structure at the termination of first-stage boost. The data were used as inputs for analyses of structural and thermal stress, which were performed to assess the structural adequacy of the SLA for the AS-503 and subsequent spacecraft.

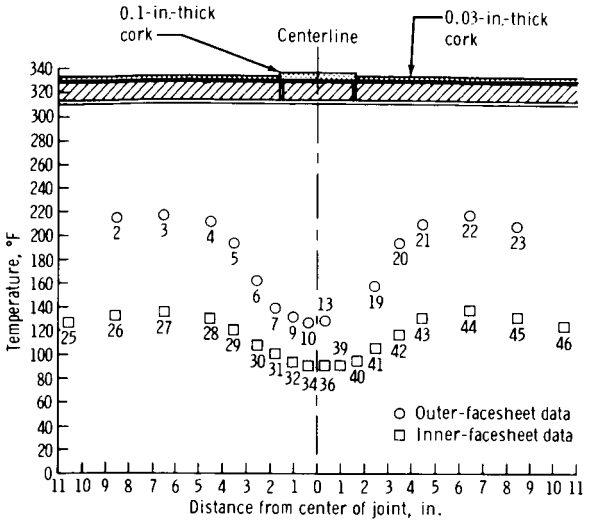

Figure 26. - Temperature distribution for test joint 3 covered with an AS-503 cork pattern and subjected to an AS-503 trajectory simulation.

Flight Data for the SM and SLA as Compared with Analytical Predictions

Spacecraft AS-202. - The temperature history for SM sensor SA7916T is shown in figure 27. The analytical predictions, which were based on the actual launch trajectory, are slightly conservative. The maximum predicted response is based on full solar exposure on the panel and radiation cooling to the earth; the minimum predicted response is based on no solar exposure or radiation cooling to space. The maximum and minimum predictions should bracket the expected response. The temperature history and predicted responses for SLA sensor AA7931T are shown in figure 28. The spike in the measured data at an elapsed time of 145 seconds was caused by the heating from the forward-firing retrorockets of the first stage at separation; this heating was not accounted for in the analysis. The temperature history and analytical predictions for SLA inner-surface sensor AA7932T are shown in figure 29. As observed in the radiant-heating tests, the analytical predictions were higher than the actual temperatures encountered on the SLA

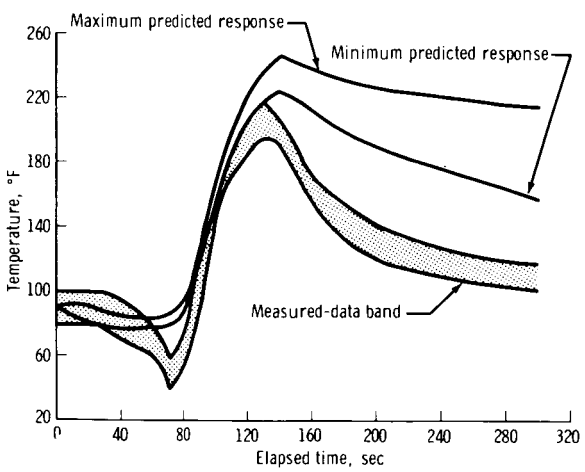

Figure 27. - Temperature history for SM sensor SA7916T (outer surface, X_S = 350 in., and a circumferential position of 253°) during the launch of spacecraft AS-202.

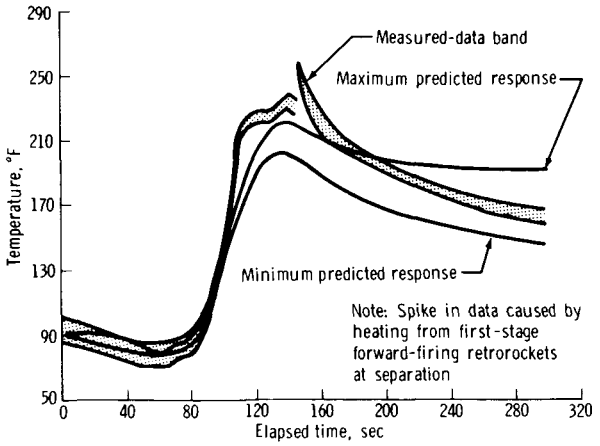

Figure 28. - Temperature history for SLA sensor AA7931T (outer surface, X_A = 775 in., and a circumferential position of 124°) during the launch of spacecraft AS-202.

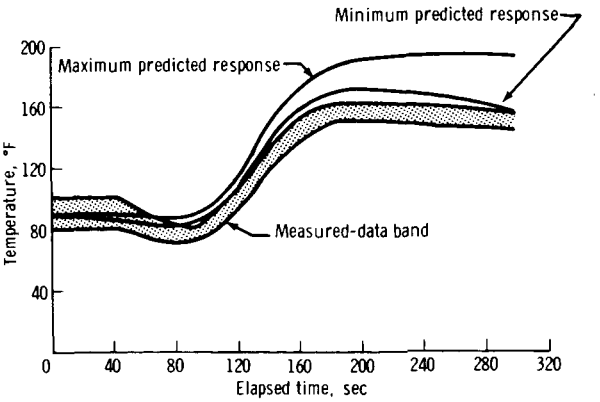

Figure 29. - Temperature history for SLA sensor AA7932T (inner surface, X_A = 775 in., and a circumferential position of 124°) during the launch of spacecraft AS-202.

inner surface. The higher predictions probably were caused by the adiabatic-inner-surface assumption that was made for all the analytical predictions.

Spacecraft AS-501. - The majority of the SM surface was covered with cork for the Apollo 4 mission, and only the inner surface of the SM was instrumented with thermocouples. As a result, the maximum measured temperature for the AS-501 SM during boost was 90° F. The temperature history and analytical predictions for SLA sensor AA7864T are shown in figure 30. Except for the first 80 seconds of the launch phase, the correlation is good. A review of atmospheric balloon data from the NASA John F. Kennedy Space Center indicated that the atmospheric temperature up to approximately 50 000 feet (0 to 80 seconds) was considerably colder than was indicated by the 1962 standard atmosphere (ref. 8), which was used in the analysis. The unusually cold atmospheric conditions resulted in an initial cooling after lift-off.

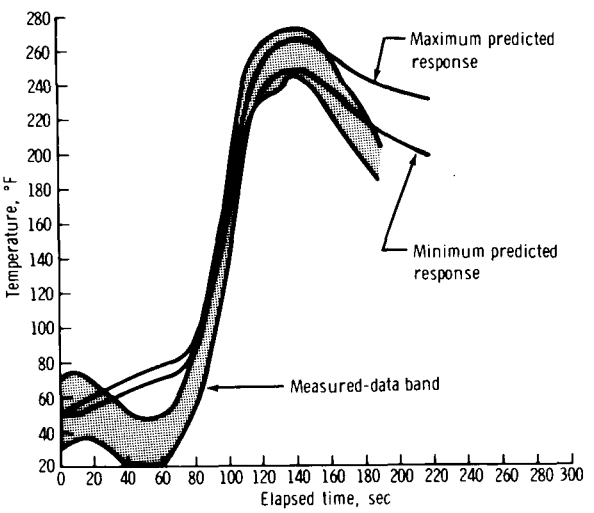

Figure 30. - Temperature history for SLA sensor AA7864T (outer surface, X_A = 730 in., and a circumferential position of 174°) during the launch of spacecraft AS-501.

CONCLUDING REMARKS

The analytical capabilities for predicting spacecraft heating characteristics and structural temperatures were adequate for prediction of the Apollo spacecraft temperatures during boost. Given the pressure distribution over the surface of the vehicle, the analytical techniques provided reasonably accurate predictions of the heating rates and thermal responses of the spacecraft during boost. For areas of the spacecraft having local pressure disturbances, the utilized techniques had dubious value. Pressure disturbances, caused by external hinges, umbilicals, RCS modules, et cetera, result in localized areas of higher heating. For the SM and SLA, the problem of protuberance-affected areas was solved by applying an experimentally determined heating-rate factor to the smooth-body heating rates. The analytical predictions resulting from this procedure were overly conservative for the Apollo-type protuberances.

In the future, to reduce the thermal-protection weight penalty associated with overconservatism, attention should be given to obtaining better techniques for predicting the effect of protuberance heating on spacecraft. The use of protuberance factors that are functions of Mach number should eliminate much of the overconservatism. Although the techniques that were used for design of the boost thermal protection system for the Apollo spacecraft were conservative (because no structural element or component exceeded the design temperature), the Apollo 6 (AS-502) anomaly led to increased thermal protection of the SLA. This addition was made to increase the structural margins and to reduce thermal stresses below the originally defined requirements. The analytical-prediction and testing techniques that were developed for the Apollo Program should enable the thermal analyst to design future spacecraft with less severe thermal gradients in the structure during boost and with lighter weight boost thermal protection systems.

Manned Spacecraft Center
National Aeronautics and Space Administration
Houston, Texas, October 26, 1972
914-50-20-12-72

REFERENCES

1. Anon.: Thermal Data Apollo Block II Spacecraft. Vol. I, Structural Thermal Response, SD 67-1107, secs. I to IV, Space Div., N. Am. Rockwell Corp., Nov. 20, 1968.

2. Eckert, E. R. G.: Engineering Relations for Friction and Heat Transfer to Surfaces in High Velocity Flow. J. Aeron. Sci., vol. 22, no. 8, Aug. 1955, pp. 585-587.

3. Blasius, H.: Grenzschichten in Flüssigkeiten mit Kleiner Reibung. Z. Math. U. Phys. vol. 56, 1908, pp. 1-37. (Available as NACA TM 1256.)

4. F. Schutz-Grunow: A New Resistance Law for Smooth Plates. Luftfahrt Forsch., vol. 17, 1940, pp. 239-246. (Available as NACA TM 986.)

5. Anon.: Thermal Data Apollo Block II Spacecraft. Vol. II, Aerodynamic Heating Environment, SD 67-1107, Space Div., N. Am. Rockwell Corp., July 1, 1968.

6. Burbank, Paige B.; Newlander, Robert A.; and Collins, Ida K.: Heat-Transfer and Pressure Measurement on a Flat-Plate Surface and Heat-Transfer Measurements on Attacked Protuberances in a Supersonic Turbulent Boundary Layer at Mach Numbers of 2.65, 3.51, and 4.44. NASA TN D-1372, 1962.

7. Anon.: Evaluation of the Thermal Properties of Materials. Vol. II, Data Handbook Final Report, AVSSD 0197-66-RR, Space Systems Div., Avco Corp., June 28, 1966.

8. Anon.: U. S. Standard Atmosphere, 1962. U. S. Govt. Printing Office.